Saudi Journal of Biological Sciences (2016) 23, S22–S31

King Saud University

Saudi Journal of Biological Sciences

www.ksu.edu.sa
www.sciencedirect.com

ORIGINAL ARTICLE

One-step synthesis of interpenetrating network hydrogels: Environment sensitivities and drug delivery properties

Jingqiong Lu [a], Yinhui Li [a], Deng Hu [a], Xiaoling Chen [a], Yongmei Liu [a], Liping Wang [b], Muhammmad Aqeel Ashraf [c,d], Yansheng Zhao [a,*]

[a] College of Chemistry and Chemical Engineering, Taiyuan University of Technology, Taiyuan 030024, China
[b] Sansom Institute for Health Research, School of Pharmacy and Medical Sciences, University of South Australia, Adelaide 5001, Australia
[c] Department of Geology, Faculty of Science, University of Malaya, 50603 Kuala Lumpur, Malaysia
[d] Faculty of Science & Natural Resources, Universiti Malaysia Sabah, 88400 Kota Kinabalu, Sabah, Malaysia

Received 12 June 2015; revised 14 June 2015; accepted 15 June 2015
Available online 19 June 2015

KEYWORDS

Poly(aspartic acid);
Carboxymethyl chitosan;
IPN;
Hydrogel;
Drug release

Abstract A novel interpenetrating network hydrogel for drug controlled release, composed of modified poly(aspartic acid) (KPAsp) and carboxymethyl chitosan (CMCTS), was prepared in aqueous system. The surface morphology and composition of hydrogels were characterized by SEM and FTIR. The swelling properties of KPAsp, KPAsp/CMCTS semi-IPN and KPAsp/CMCTS IPN hydrogels were investigated and the swelling dynamics of the hydrogels was analyzed based on the Fickian equation. The pH, temperature and salt sensitivities of hydrogels were further studied, and the prepared hydrogels showed extremely sensitive properties to pH, temperature, the ionic salts kinds and concentration. The results of controlled drug release behaviors of the hydrogels revealed that the introduction of IPN observably improved the drug release properties of hydrogels, the release rate of drug from hydrogels can be controlled by the structure of the hydrogels and pH value of the external environment, a relative large amount of drug released was preferred under simulated intestinal fluid. These results illustrated high potential of the KPAsp/CMCTS IPN hydrogels for application as drug carriers.

1. Introduction

Due to their inherited abundant strong hydrophilic groups such as carboxyl and low cross linking three dimensional network structures, hydrogels are paid extensive attention as promising water swelling functional polymer materials (Mehr et al., 2009). They can absorb hundreds or thousands of times

* Corresponding author.
E-mail address: zhaoyansheng@tyut.edu.cn (Y. Zhao).
Peer review under responsibility of King Saud University.

Production and hosting by Elsevier

http://dx.doi.org/10.1016/j.sjbs.2015.06.012
1319-562X © 2015 Production and hosting by Elsevier B.V. on behalf of King Saud University.

of deionized water than themselves, meanwhile maintaining their three-dimensional network structure in insoluble state (Juby et al., 2012). At present, most hydrogels are based on acrylic acids, such as acrylamide and poly(acrylic acid) (Ruiz-Rubio et al., 2014), chitosan–acrylic acid (Gyarmati et al., 2014), poly(acrylic acid), poly(4-vinylpyridine) (Ge and Wang, 2014) etc. They are inferior to salt tolerance and non biodegradable that greatly limits their applications. Recently, poly aspartic acids have been widely studied because they have excellent properties such good biocompatibility, biodegradability, being nontoxic and environmentally harmless, etc. (Li et al., 2014). Poly(aspartic acid) hydrogels appear interesting for their biological and pharmaceutical applications because of their protein like structure and thermo-, pH- sensitivities (Liu et al., 2010; Matsuyama et al., 1980). Nevertheless, pure poly aspartic acid still exists in a simple structure and has poor salt tolerance. Instead, carboxymethyl chitosan (CMCTS), a water-soluble derivative of chitosan, has admirable biocompatibility (Chen et al., 2002), excellent biodegradability, and high moisture retention capacity (Chen et al., 2004). In particular, CMCTS contains a large amount of hydroxyl which can improve the salt resistance of polymers.

Interpenetrating polymer networks i.e., IPN are capable of combining 2–3 polymers to form a cross link network. Many studies have proven that IPN can greatly enhance the compatibility among the components and in turn ameliorate the network structures. They include gelatin/alginate (Hu et al., 2015) natural rubber/cassava starch (Mandal and Ray, 2014), chitosan/acrylic copolymer (Vudjunga et al., 2014), salecan/poly (N,N-dimethylacry lamide-co-2-hydroxyethyl methacrylate) (Hu et al., 2014), and acrylamide and potato starch (Dragan and Apopei, 2013). Typical swelling equilibrium IPN hydrogel can undergo a volume change with the small changes of environmental factors, e.g., temperature, pH, and ionic strength (Ashraf et al., 2013; Batool et al., 2015; Li et al., 2007), which is called environment sensitivity. Take an example of pH sensitivity, as an important role of the human body, it has gained great attention for its potential applications in oral drug controlled release systems. Moreover, in previous preparation methods exist several problems such as complex, asymmetric distribution, low effectiveness, etc. In particular, there is seldom address of preparation in an aqueous system. In this study, a simple one-step method was adopted to synthesize modified poly (aspartic acid) and carboxymethyl chitosan interpenetrating network (KPAsp/CMCTS IPN) hydrogels in an aqueous system.

2. Materials and methods

The novel KPAsp/CMCTS hydroxyls with semi-INP and IPN structures were prepared. The swelling properties and salt, temperature and pH-sensitivities of KPAsp, KPAsp/CMCTS semi-IPN and KPAsp/CMCTS IPN hydrogels were investigated The cross-linking structure and swelling properties of KPAsp, KPAsp/CMCTS semi-IPN and KPAsp/CMCTS IPN hydrogels were proved by FTIR, SEM and tea-bag methods. Their sensitivity characteristics to pH, temperature and salts were also investigated. Furthermore, the drug release properties of the KPAsp, KPAsp/CMCTS semi-IPN and KPAsp/CMCTS IPN hydrogels have been studied.

N,N-dimethylformamide (DMF), Ethanol absolute were purchased from Tianjin Kemiou Chemical Regent Company, China. Glutaraldehyde, 3-aminpropyltriethoxysilane (KH-550), Sodium chloride (NaCl) and Sodium hydroxide (NaOH) were obtained from Tianjin Fengfan Technology Chemical Regent Company Ltd., China. Ferric trichloride and anhydrous calcium chloride were procured from Tianjin Damao Chemical Regent Company Ltd., China. All reagents were of analytical grade. CMCTS was provided by the Nanjing Chemical Industry. Polysuccinimide (PSI) was prepared in our laboratory (Rajapakse et al., 2005).

The novel hydrogels were prepared by KPAsp and CMCTS in aqueous solution. The KPAsp/CMCTS semi-IPN and IPN hydrogels were complied with the cross-linking reaction mechanism, as illustrated in Fig. 1.

1 g of PSI and 10 ml DMF were simultaneously put in a 100 ml beaker under magnetic stirring at 35 °C. After PSI was completely dissolved, an amount of 1.8 mol% of KH-550 (based on PSI) was added into the solution and maintained for 3 h. The alcohol washing procedure lasted three times. Subsequently the precipitate was separated by filtration and dried at 50 °C in a vacuum oven. The KH-550 grafted PSI was then obtained.

1 g KPSI was dispersed into 20 ml deionized water. Then NaOH with a concentration of 2 mol/l was dropwise added to execute the hydrolysis reaction till the pH value reaches 10. This procedure lasted about 4 h. The product was kept in a vacuum oven at 75 °C for further reaction for another 2 h. After that, the final product was separated by alcohol filtration, dried and milled at 50 °C. The KPAsp hydrogel was then obtained.

Similarly, 1 g of KPSI was dispersed into 20 ml deionized water. Then 24.5 ml aqueous solution of CMCTS (containing 0.6 g CMCTS) was poured into the KPSI solution with agitation and heated to 35 °C. Next, NaOH (with a concentration of 2 mol/l) was added drop-wise into the solution to maintain the pH at 10 for 4 h. Half an hour before hydrolysis reaction completed, the cross-linker, glutaraldehyde (4.2 mol% based on CMCTS) was added. The solution was put in a vacuum oven at 75 °C for further reaction for 2 h. Afterward, alcohol was added to the solution, the precipitate was separated by filtration and dried at 50 °C in a vacuum oven. Thereby the KPAsp/CMCTS IPN hydrogel was obtained. KPAsp/CMCTS semi-IPN hydrogel was also prepared in the same manner without the addition of glutaraldehyde.

FTIR spectra were recorded on a Shimadz-8400S FTIR instrument (Japan) in the range of 500–4000 cm^{-1} with a resolution of 2 cm^{-1}. The vacuum-dried samples of KPAsp, semi-IPN, and IPN hydrogel were dispersed in potassium bromide (KBr) pellets.

The surface and morphologies of different hydrogels were examined using SEM (MIRA3, UK). Samples were sectioned into slices and mounted on aluminum stubs, using a double-sided adhesive tape. The samples were then directly visualized by SEM at an accelerating voltage of 10 kV after sputter-coating with an ultrathin layer of gold.

Thermogravimetry analysis (TGA) was carried out on a TGA-50 Shimadzu instrument (Japan), over a temperature range of 40–600 °C. The heating rate was 10 °C min^{-1} and the nitrogen flow rate was 100 ml min^{-1}.

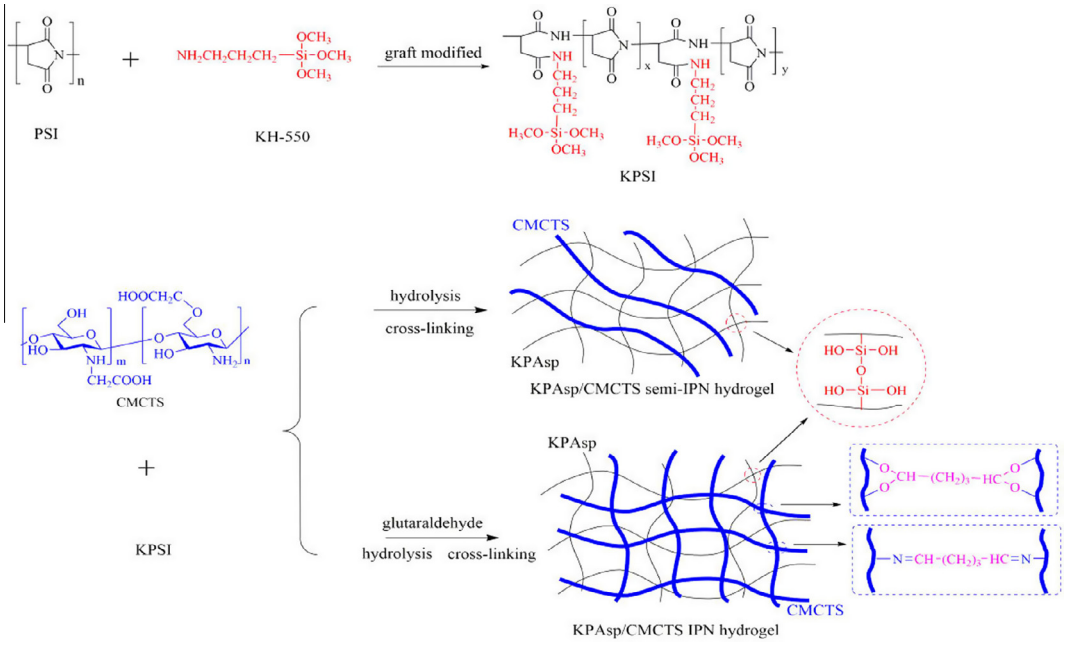

Figure 1 Schematic of KPAsp/CMCTS semi-IPN and IPN hydrogel preparation.

Swelling behavior of the hydrogels was examined by placing 0.1 g (precision of 0.001 g) of the hydrogel into the tea-bag that was made of nylon wire mesh. Then the tea-bag was fully immersed in excess distilled water or physiological saline at 30 °C for a predetermined time interval. Then the tea-bag with swollen hydrogels was suspended in the air for 15 min to remove the surface water of hydrogels before weighing on a balance. The swelling ratio of the hydrogel was given by Eq. (1) (Lai and Li, 2011):

$$Q = \frac{W_s - W_d}{W_d} \tag{1}$$

where, Ws and W_d represent the weights of the swollen hydrogel and the dried sample, respectively, (g/g). In this paper, Q_d is the swelling in distilled water and Q_s is the swelling ratio in physiological saline.

Effect of pH on swelling behaviors of the hydrogels was also investigated. The desired pH of buffer solutions was adjusted by HCl (1 mol/l) and NaOH (1 mol/l) solution, the pH values were precisely measured on a pH-meter (METTLER TOLEDO, China). The dried samples were immersed for 24 h in the solution of different pH values from 2 to 12 at 30 °C to reach equilibrium. The equilibrium swelling ratio was calculated by Eq. (1).

25 mg of Salicylic acid was precisely weighed, dissolved in 100 ml deionized water, then 0.2 ml, 0.4 ml, 0.6 ml, 0.8 ml, 1.0 ml of that solution was diluted with 50 ml deionized water. The absorbance of each solution was measured at the maximum absorption wavelength of 300 nm. UV spectra were collected using a UV spectroscopy (UV-1700 Hitachi High Technologies, Tokyo). The absorbance standard curve of salicylic acid for different concentrations was obtained and shown in Fig. 2, the standard equation was calculated as $A = 0.0057 + 53.1C$ (A = absorbance and C = concentration).

Salicylic acid was chosen as a model drug for drug absorption and release experiments. 0.5 g of dry hydrogel was soaked

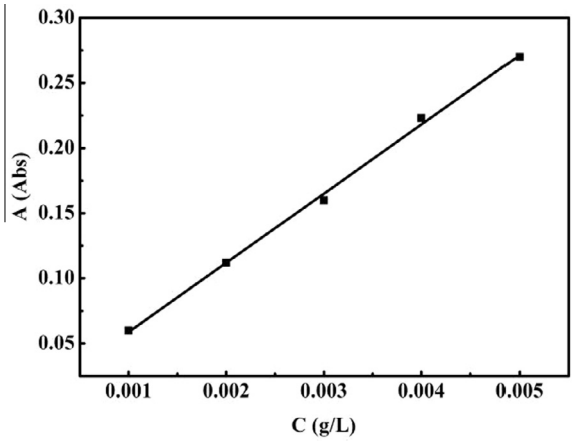

Figure 2 Standard curve of salicylic acid.

in 1000 ml salicylic acid solutions (with a concentration of 1 g/L) at room temperature for 24 h and rinsed with deionized water. To measure the total amount of loaded drug, each drug-loaded hydrogel was filtered out by nylon (300 mesh). The residual volume of the filtrate was exactly measured and salicylic acid amount was estimated from the absorbance at 300 nm. UV spectra were collected using a UV spectroscopy (UV-1700 Hitachi High Technologies, Tokyo).

The drug-loaded samples were immersed in buffer solutions of pH 1.2 (simulated gastric fluid) and 7.4 (simulated intestinal fluid) at 37 °C to evaluate the drug release from drug-loaded hydrogels. The amount of salicylic acid released into different pH solutions was periodically monitored by following the UV absorption of salicylic acid in the external solution. The concentration of salicylic acid was calculated by using a salicylic acid standard curve. Salicylic acid release amount was calculated by the following equation, the results were represented via a sustained-release rate:

$$\text{Drug release } (\%) = C(t)/C(0) \times 100 \quad (2)$$

where, $C(0)$ and $C(t)$ are the amount of drug loaded and released at time t, respectively.

3. Results and discussion

The FTIR spectrum (Surhio et al., 2014; Safi et al., 2015) of KPAsp (a), KPAsp/CMCTS semi-IPN (b) and KPAsp/CMCTS IPN (c) hydrogels are shown in Fig. 3. In curve (a), the strong broad band at 3416 cm^{-1} is due to O–H stretching, while the amidocyanogen (N–H) stretching also appears in place. The bands at 1648 and 1397 cm^{-1} are related to the symmetric and asymmetric stretching vibrations of C═O, respectively. The peak at 1081 cm^{-1} can be ascribed to the symmetric stretching vibrations of Si–O–Si that was formed through KPAsp self crosslinking. These were characteristic absorptions in KPAsp structures. Compared with (a), the appearance of 1223 cm^{-1} in curve (b) represented the stretching absorption peak of C–O–C, this could be attributed to the introduction of CMCTS. The band at 1223 cm^{-1} shifted to 1210 cm^{-1} in curve (c), this maybe owing to the additional ether link generated by the cross linking reaction of glutaraldehyde with CMCTS. All the above indicated the semi-IPN and the IPN structures of KPAsp and CMCTS had been formed.

Fig. 4 shows the SEM images of KPAsp (a), KPAsp/CMCTS semi-IPN (b) and KPAsp/CMCTS IPN (c) hydrogels. It is obvious that the surface of the KPAsp hydrogel (Fig. 4a) is smooth, the semi-IPN (Fig. 4b) exhibited a comparatively loose and coarse surface, while the surface morphology of IPN (Fig. 4c) hydrogels was more rough and porous. The surface roughness and pore densities of IPN hydrogels were the highest among the three samples. This observation revealed the structure of polymer could be adjusted by the IPN process, which in turn improves the pore and surface morphology of the hydrogels, these pores as transport channels provide a convenient way to improve the hydrogel swelling. This means the IPN structure is helpful to increase in the equilibrium swelling rate due to the effects of capillary imbibition and enlarged specific surface area in the hydrogel.

In order to understand and investigate the thermal behavior of KPAsp (a), KPAsp/CMCTS semi-IPN (b) and KPAsp/CMCTS IPN (c) hydrogels, the three samples were tested by TGA. As can be seen in Fig. 5, the three samples had a small quantity of weightlessness below 250 °C, which corresponded to the surface moisture and bound water evaporation. At 281 °C and 293 °C, the semi-IPN hydrogels and IPN hydrogel thermally decomposed, whereas thermal decomposition of the KPAsp hydrogel took place at 254 °C. The thermal decomposition temperature for KPAsp sample is much lower than that of semi-IPN and IPN hydrogels, which indicated that IPN structure significantly improved the thermal stabilities of hydrogels. This phenomenon can be expressed due to the interaction between the KPAsp chains being weak, and in the semi-IPN structure, the CMCTS chains were dispersed into the network of KPAsp, the semi-IPN sample is not easy to decompose because of constraint of hydrogen bonds. Moreover, though CMCTS chains in the IPN sample tends to form a network structure through cross-linking of glutaraldehyde, the second network structure leads to the thermal stabilities of the IPN hydrogel.

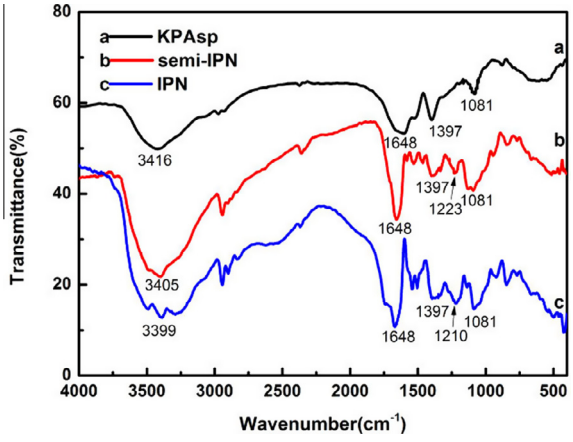

Figure 3 FTIR spectrum of the hydrogels: KPAsp (a), KPAsp/CMCTS semi-IPN (b) and KPAsp/CMCTS IPN (c).

The swelling behavior of KPAsp, semi-IPN and IPN CMCTS/KPAsp hydrogels in distilled water and physiological saline are shown in Fig. 6. The measured swelling ratios of KPAsp, semi-IPN and IPN CMCTS/KPAsp hydrogels are 180.31, 236.5 and 306.7 g/g respectively. The IPN structure has the maximal swelling ratio. The results clearly indicate IPN or semi-IPN is beneficial to the increase of swelling capacity. In general, the increase of swelling rate is ascribed to the more contact probability of the active particles and polymer. In the case of semi-IPN KPAsp/CMCTS hydrogels, CMCTS as a large molecular with a long chain impenetrate into the cross link network of KPAsp. Three hydrophilic groups ($–NH_2$, –OH and –COOH) contained in CMCTS could be produced during this process. The swelling behavior was improved via coordinate effects between these groups. In physiological saline, the swelling ratios of semi-IPN and IPN KPAsp/CMCTS hydrogels are measured to be 66.2 and 98.1 g/g, which increased 104 wt% and 203 wt% than that of the KPAsp hydrogel. This phenomenon can be ascribed to the non ion type hydrophilic group –OH coordinates with the anion group –COONa. As a result, the identical ion effect and salt effect are weakened, which makes the swelling rate of KPAsp/CMCTS semi-IPN higher than that of KPAsp. In addition, for the KPAsp/CMCTS IPN hydrogel, the large molecular chains in CMCTS were cross linked by the ether bond to form a second network structure. At the same time, the amount of hydrophilic groups further increase and the coordinate effect strengthens as well. Thus the penetrating pressure in the dual network increases in physiological saline. Consequently, the swelling rate for the IPN structure both in distilled water and 0.9 wt% physiological saline was increased than that of KPAsp/CMCTS semi-IPN.

The swelling behavior of hydrogels is closely related to the diffusion of water molecules and the expansion of the polymer network. There are many factors influencing the water diffusion mode and the rate of the hydrogel, including stress relaxation of polymer, crosslink concentration and ionic groups on polymer networks (Naureen et al., 2014; Khaskheli et al., 2015). In order to precisely understand the swelling mechanism, the swelling behavior of hydrogels was fitted to the following equation (Kiyani et al., 2014):

$$F = \frac{M_t}{M_{\inf}} = kt^n \quad (3)$$

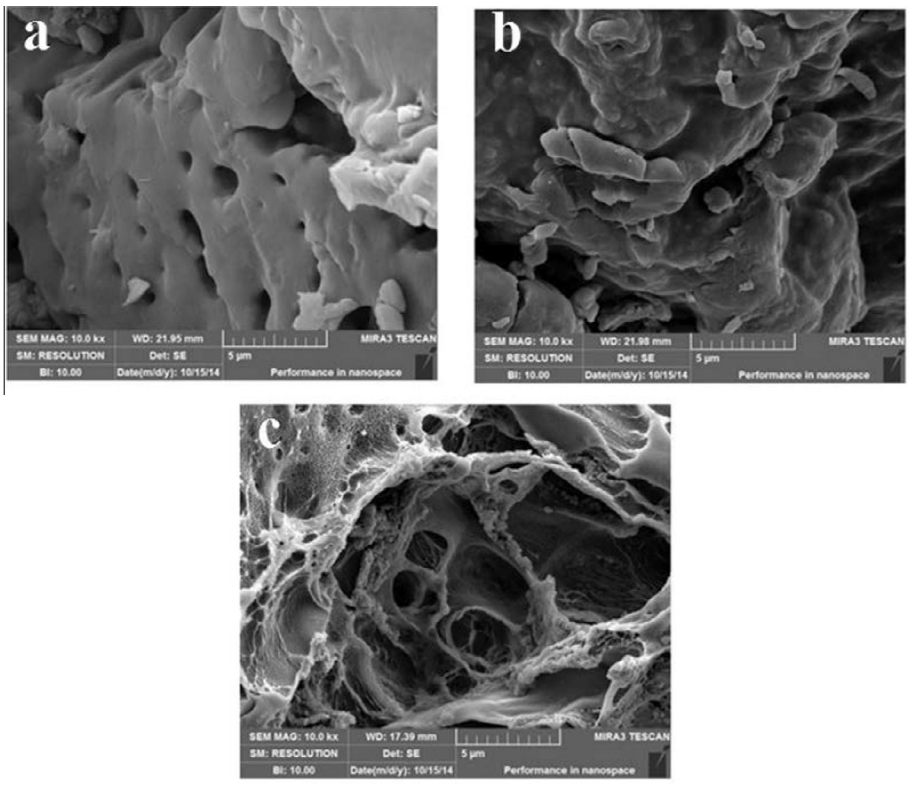

Figure 4 SEM images of KPAsp (a), KPAsp/CMCTS semi-IPN (b) and KPAsp/CMCTS IPN (c) hydrogels.

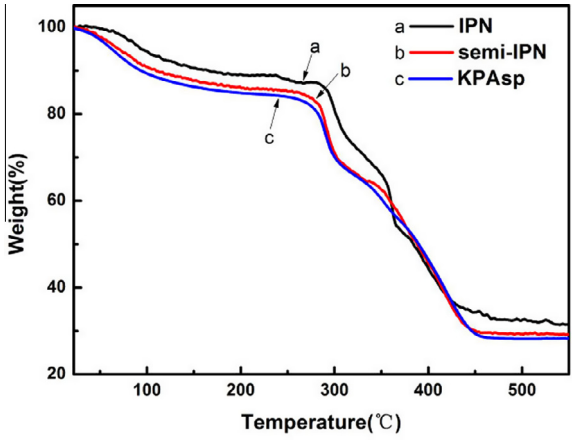

Figure 5 TGA patterns of KPAsp (a), KPAsp/CMCTS semi-IPN (b) and KPAsp/CMCTS IPN (c) hydrogels.

where, M_t and M_{inf} denote the amount of water diffused into the hydrogel at time t, and infinite time (at equilibrium), respectively; k is a kinetic constant and n is swelling exponent which can interpret the type of water diffusion. For sample, Fickian diffusion, which appears when polymer chains have high mobility, corresponds to $n < 0.5$, whereas $0.5 < n < 1.0$ the diffusion follows non-Fickian diffusion, where anomalous transport (coupling of Fickian diffusion and polymer relaxation/degradation) is observed. lnF as the function of lnt for the swelling within the initial one hour was depicted in Fig. 7. It can be seen that they have a simple linear relationship. The exponent n can be calculated from the line slope. To simplify, we summarized the swelling kinetic parameters in Table 1. Obviously, the water diffusion behavior of the KPAsp hydrogel follows the Fickian diffusion mechanism, while the water diffusion behavior of semi-IPN and IPN hydrogels follows the non-Fickan diffusion controlled mechanism. This result is owing to the fact that the increased pore density and surface area in semi-IPN and IPN hydrogels facilitate the diffusion water molecular, the hydrogel swelling process is controlled by Fickian diffusion and expansion of the large molecular chains.

The swelling behaviors of KPAsp, semi-IPN and IPN CMCTS/KPAsp hydrogels in solution with a pH range of 2–12 at 30 °C are illustrated in Fig. 8. It can be seen that the swelling ratio reaches to maximum when pH = 4 and 9. The swelling rate has a mild flattening in the pH range of 5–8. We attributed this to the different electron conductor conditions under various pH values in the IPN structure. During the swelling process, there exist abundant active groups including carboxyl, carbonyl and amino in the three-dimensional network structure, the electron conductor distribution was aroused from the interactions of different electric charges. When pH < 4, the main electric group is protonated $-NH_2^+$. The repulsion force and increased hydrophilicity induces the increase of the swelling rate. While pH locates at a range of 4–9, a joint reaction from ion bondings between $-NH_2$ and –COOH, and hydrogen bond between –COOH and –OH promotes a dense structure, which leads to a reduced swelling capacity. The reason for the maximum swelling rate at pH = 9 may be expressed by the reaction cross linking of CMCTS chains via glutaraldehyde during the formation of the IPN network. The close structure between the chains was

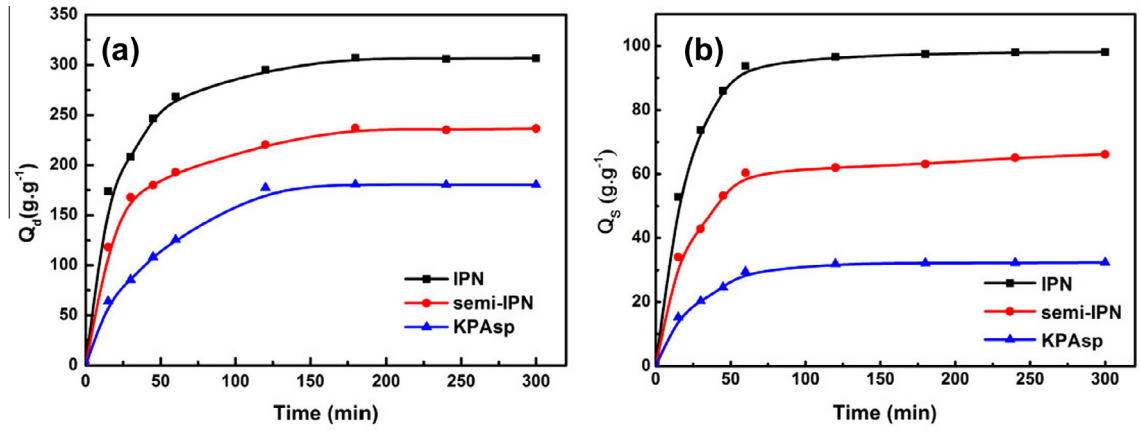

Figure 6 Swelling ratios of KPAsp, KPAsp/CMCTS semi-IPN and KPAsp/CMCTS IPN hydrogels in distilled water (a) and 0.9 wt% physiological saline (b).

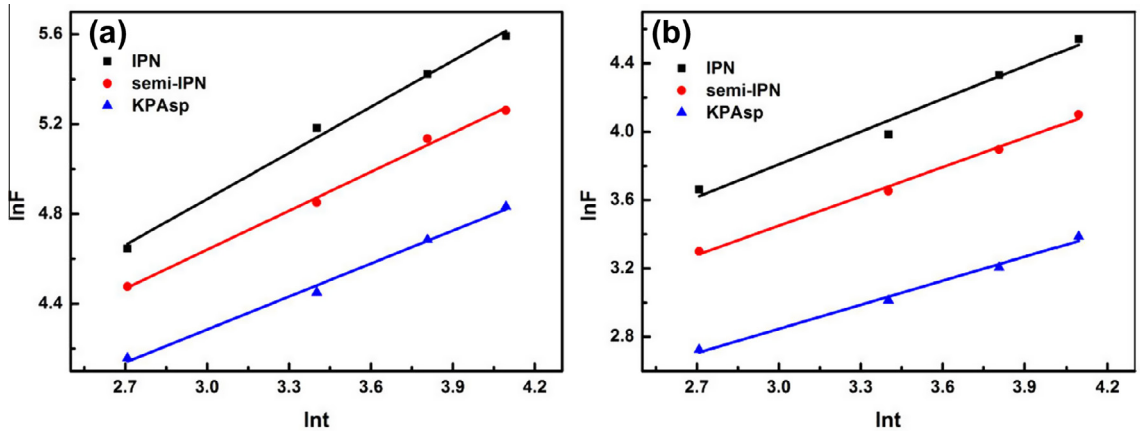

Figure 7 Swelling kinetics (lnt–lnF fitting curve) of KPAsp, KPAsp/CMCTS semi-IPN and KPAsp/CMCTS IPN hydrogels in distilled water (a) and in 0.9 wt% physiological saline (b).

Table 1 Swelling kinetic parameters n, k and R^2 for lnt–lnf.

Diffusion medium	Sample	n	k	R^2
Distilled water	KPAsp	0.4895	2.8166	0.9917
	Semi-IPN	0.5784	2.9055	0.9941
	IPN	0.6843	2.814	0.9919
Physiological saline	KPAsp	0.4691	1.4393	0.9889
	Semi-IPN	0.5715	1.6429	0.9926
	IPN	0.6379	1.8951	0.9695

profitable to the diastolic of KPAsp chains. Furthermore, according to the Donnan equilibrium theory, the swelling of the hydrogel is mainly determined by the penetrating pressure induced by the concentration difference of free ions in and outside the hydrogel. When pH < 4, the main electronic group in hydrogels is protonated $-NH_2^+$, while for pH > 9, the main electronic group is unprotonated $-COO^-$. In the pH range of 4–9, the concentration of free ion inside the hydrogel is larger than that of the environment. Hence the swelling behavior of the hydrogel occurs to reduce the electron charges inside the hydrogel. When pH ranges from 5 to 8, the electric charges

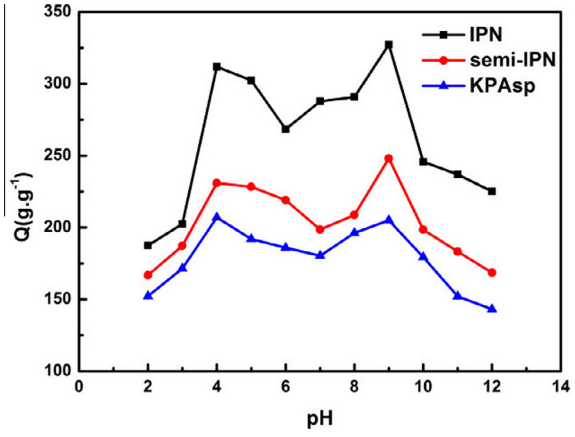

Figure 8 Swelling ratios of KPAsp, KPAsp/CMCTS semi-IPN and KPAsp/CMCTS IPN hydrogels under different pH values.

of $-COO^-$ and $-NH_2^+$ in KPAsp/CMCTS are quite equal, hence the concentration difference of free ions is almost zero due to the nearly equal electrostatic attraction. The hydrogel was thus dehydrated and shrank adapting to the external penetrating pressure.

The effect of salt solutions on the swelling ratio of the prepared hydrogels with different structures is shown in Fig. 9(a–c), corresponding to the result of $FeCl_3$, $CaCl_2$ and NaCl solution, respectively. It is observed that the swelling ratios of prepared hydrogels decrease with the increase of salt concentration. This is due to the fact that the ionic strength of the solution increases with the boosting of the solution concentration. During the swelling process, the anion charge groups on hydrogels are first ionized. Then the surface swells due to the electrostatic repulsion between adjacent ionized groups. However, with ionic strength continuously increasing, the anionic groups on the hydrogels are screened by the cations in solution. So the swelling ratio decreases with the further increase of ionic strength. Another possible contribution to this phenomenon is that Cl^- outside the solution swamps the negatively charged carboxylic groups.

We can also find that the swelling abilities of hydrogels are different in salt solutions with different cationic kinds. At the same concentration of the three chloride salt solutions ($FeCl_3$, $CaCl_2$ and NaCl), the swelling ratios of hydrogels decrease with the increase of the charge of the cation by reason of the ionic strength increasing with the increase of the charge of the cation. The relationship between the swelling ratio and the ionic strength in 10 mmol/l salt solution is shown in Table 2.

In addition to the cause of the ionic strength, the complexation between the multivalent cations and the –COOH groups on the polymer chain generates ionic cross-linking in the hydrogels. With the increase of the cation charge, the ionic cross-linking increased gradually. As a result, the conformation of the hydrogel was changed from an expanded structure to a more compact matrix. According to the Flory's theory (Flory, 1953; Butt et al., 2015), the swelling ratio decreases with the further intensive crosslinking density in the hydrogels.

At the same ionic strength for a given salt solution, the swelling ratio of the IPN hydrogel has the highest value, which demonstrates that the IPN structure could improve the salt tolerance of hydrogels. There were two reasons for the high swelling ratio of the IPN hydrogel. Complexations between multivalent cations and –COOH groups are weakened due to the introduction of the hydrophilic group –OH and $–NH_2$ and the construction of the second network structure comprised of crosslinked CMCTS, which increased the effective network structure of hydrogels.

Swelling rates of KPAsp, KPAsp/CMCTS semi-IPN and KPAsp/CMCTS IPN hydrogels with variations of temperature are shown in Fig. 10. The swelling ratio of semi-IPN and IPN hydrogels is always higher than that of the KPAsp hydrogel. It can also be seen that for all the three samples, the swelling rate was first increased with the argument that the temperature then falls down quickly to a low swelling level. The temperature of optimum swelling ratio for prepared samples is 40 °C. That can be explained as the interaction of molecular bondings with the network structure. As mentioned previously, strong

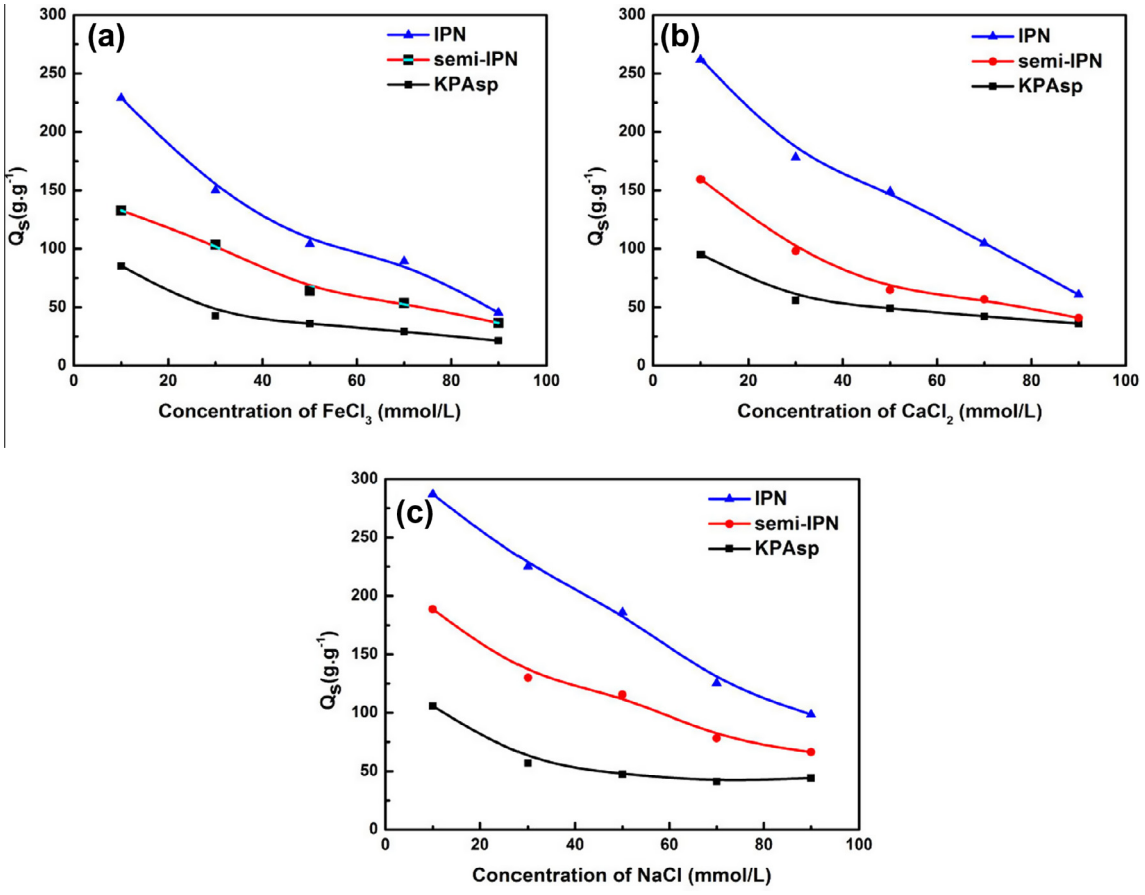

Figure 9 Swelling ratios of KPAsp, KPAsp/CMCTS semi-IPN and KPAsp/CMCTS IPN hydrogels in different salt solutions: $FeCl_3$ (a), $CaCl_2$ (b) and NaCl (c).

Table 2 Relationship between the ionic strength and swelling ratio.

Solution	Ionic strength (mmol/kg)	Swelling ratio (g/g)	
		IPN KPAsp/CMCTS	Semi-IPN KPAsp/CMCTS
10 mmol/l NaCl solution	10	286.95	188.67
10 mmol/l $CaCl_2$ solution	30	261.74	159.35
10 mmol/l $FeCl_3$ solution	60	228.83	132.74

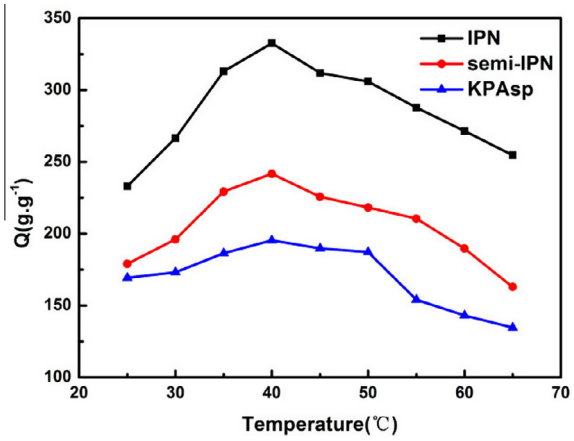

Figure 10 Swelling ratios of KPAsp, KPAsp/CMCTS semi-IPN and KPAsp/CMCTS IPN hydrogels with variations of temperature.

hydrogen bondings were produced between the carboxyl, hydroxyl, and imide groups in the polymer molecular chains. The introduction of CMCTS into the hydrogel can efficiently enhance the number of hydroxyl groups which is of benefit to strengthen intermolecular forces. If the hydrogel was put at low temperature, these hydrogen-bonds compress the network structure to shrinking and bending status. The molecular chains have little chance to contact with the water molecular, which results in a minor swelling rate. As the temperature increases, the hydrogen-bond effects were weakened and the twisted polymer molecular chains were torn up gradually. As a consequence, their contact probability with water molecular grows larger, thus the swelling ratio increases slowly. However, when the temperature is too high, the molecular chains would be destroyed even decomposed. The swelling rate was therefore decreased rapidly due to the damage of the network structure.

The measured amounts of salicylic acid loaded in KPAsp, KPAsp/CMCTS semi-IPN and KPAsp/CMCTS IPN hydrogels were 36.69 mg/g, 54.36 mg/g and 72.07 mg/g, respectively. The more amounts of salicylic acid loaded in the KPAsp/CMCTS IPN hydrogel attributed to the introduction of hydrophilic groups (–OH, –COOH and $–NH_2$) and the increase of an effective network structure of the IPN hydrogel. Moreover, the increased porous structure could also enhance the diffusion of the drug into the hydrogel network.

The release profiles of salicylic acid from KPAsp, KPAsp/CMCTS semi-IPN and KPAsp/CMCTS IPN hydrogels were tested at pH values of 1.2 (simulated gastric fluid) and 7.4 (simulated intestinal fluid) at 37 °C. As could be seen from Fig. 11, the release behaviors of salicylic acid from the prepared hydrogels are distinctly pH- responsible. The drug release of each hydrogel at pH values of 1.2 was obviously slower than that at pH values of 7.4. And the release rate of salicylic acid from the KPAsp/CMCTS IPN hydrogel is always the highest among the three hydrogels, which should be related to the IPN structure with increased porous structure and specific surface area. At pH 1.2 and 7.4, the corresponding cumulative amounts of salicylic acid released from the KPAsp/CMCTS IPN hydrogel were 36.9% and 62.1%, respectively. That may be ascribed as follows: Firstly, in acid environment carboxy groups on the hydrogel are in the form of –COOH, as the addition of CMCTS, –OH on the hydrogel increased, the effect of H-bonding between these –COOH and –OH limits the release of salicylic acid. Secondly, as the pH value increases, carboxy groups on the IPN hydrogel are inclined to form –COONa, the effect of H-bonding between –COOH and –OH recedes, therefore salicylic acid become easy to release from the hydrogel. Thirdly, the higher swelling ratio at the condition of pH = 7.4 than at pH = 1.2 is of benefit to

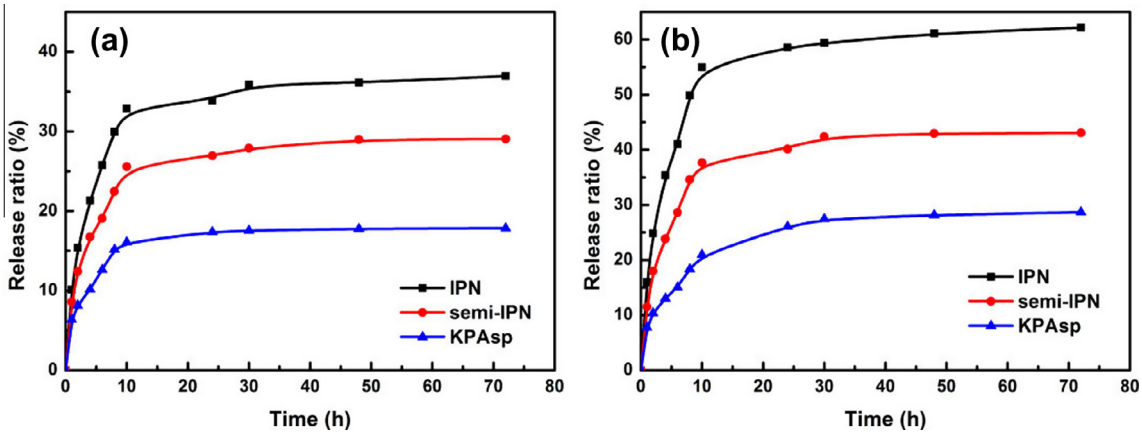

Figure 11 Release behaviors of KPAsp (a), KPAsp/CMCTS semi-IPN (b) and KPAsp/CMCTS IPN (c) hydrogels in pH values at 1.2 (a) and 7.4 (b).

drug release. In conclusion, this novel IPN hydrogel can control drug release by external surrounding stimuli and has a relative high drug release rate in simulated intestinal fluid. This would be suitable in the design and development of intestinal drug delivery systems.

A biodegradable KPAsp/CMCTS IPN hydrogel was successfully synthesized in an aqueous system using a simple one-step method. The swelling ratio, pH, temperature and salt sensitivities, drug-loaded characteristics of the KPAsp, KPAsp/CMCTS semi-IPN and KPAsp/CMCTS IPN hydrogels were investigated. The results revealed that the introduction of IPN significantly improved all the capacities of hydrogels. The maximum swelling ratio of the IPN hydrogel was 98.1 g/g in physiological saline and 306.7 g/g distilled water which showed 2 times and 70% enhancement in comparison with that of the KPAsp hydrogel. The drug controlled release properties of the prepared hydrogels were evaluated and results indicated that prepared hydrogels could control drug release by external surrounding stimuli. The drug controlled release properties of KPAsp/CMCTS IPN hydrogels is the most outstanding, and the correlative measured release profiles of salicylic acid at 37 °C were 36.9 wt% in pH = 1.2 (simulated gastric fluid) and 62.1 wt% in pH = 7.4 (simulated intestinal fluid) respectively. These studies would be exploited in the design and preparation of suitable drug delivery systems.

4. Conclusions

The results of controlled drug release behaviors of the hydrogels revealed that the introduction of IPN observably improved the drug release properties of hydrogels, the release rate of the drug from hydrogels can be controlled by the structure of the hydrogels and pH value of the external environment, a relative large amount of drug released was preferred under simulated intestinal fluid. These results illustrated the high potential of the KPAsp/CMCTS IPN hydrogels for application as drug carriers.

Acknowledgements

This work was financially supported by the Natural Science Foundation of China (Grant No. 21304066) and Scientific and Technological Projects in Shanxi Province (Grant No. 20100311117).

References

Ashraf, M.A., Ullah, S., Ahmad, I., Qureshi, A.K., Balkhair, K.S., Rehman, M.A., 2013. Green biocides, a promising technology: current and future applications. J. Sci. Food Agric. 94 (3), 388–403. http://dx.doi.org/10.1002/jsfa.6371.

Batool, S., Khalid, A., Chowdury, A.J.K., Sarfraz, M., Balkhair, K.S., Ashraf, M.A., 2015. Impacts of azo dye on ammonium oxidation process and ammonia oxidizing soil bacteria. RSC Adv. 5, 34812–34820. http://dx.doi.org/10.1039/C5RA03768A.

Butt, M.A., Ahmad, M., Fatima, A., Sultana, S., Zafar, M., Yaseen, G., Ashraf, M.A., Shinwari, Z.K., Kayani, S., 2015. Ethnomedicinal uses of plants for the treatment of snake and scorpion bite in Northern Pakistan. J. Ethnopharmacol. 1, 1–14. http://dx.doi.org/10.1016/j.jep.2015.03.045.

Chen, X.G., Wang, Z., Liu, W.S., Park, H.J., 2002. The effect of carboxymethyl-chitosan on proliferation and collagen secretion of normal and keloid skin broblasts. Biomaterials 23, 4609–4614.

Chen, S.C., Wu, Y.C., Mi, F.L., Lin, Y.H., Yu, L.C., Sung, H.W., 2004. A novel pH-sensitivehydrogel composed of N,O-carboxymethyl chitosan and alginate cross-linked by genipin for protein drug delivery. J. Controlled Release 96, 285–300.

Dragan, E.S., Apopei, D.F., 2013. Multiresponsive macroporous semi-IPN composite hydrogels based on native or anionically modified potato starch. Carbohydr. Polym. 92, 23–32.

Flory, P.J., 1953. Principles of Polymer Chemistry. Cornell University Press, Ithaca.

Ge, H.C., Wang, S.K., 2014. Thermal preparation of chitosan–acrylic acid superabsorbent: optimization, characteristic and water absorbency. Carbohydr. Polym. 113, 296–303.

Gyarmati, B., Némethy, Á., Szilágyi, A., 2014. Reversible response of poly(aspartic acid) hydrogels to external redox and pH stimuli. RSC Adv. 4, 8764–8771.

Hu, X.Y., Feng, L.D., Wei, W., Xie, A.M., Wang, S.M., Zhang, J.F., Dong, W., 2014. Synthesis and characterization of a novel semi-IPN hydrogel based on Salecan and poly (N,N-dimethylacrylamide-co-2-hydroxyethylmethacrylate). Carbohydr. Polym. 105, 135–144.

Hu, X., Lu, L.L., Xu, C., Li, X.S., 2015. Mechanically tough biomacromolecular IPN hydrogel fibers by enzymatic and ionic crosslinking. Int. J. Biol. Macromol. 72, 403–409.

Juby, K.A., Dwivedi, C., Kumar, M., Kota, S., Misra, H.S., Bajaj, P.N., 2012. Silver nanoparticle-loaded CMCTS/gum acacia hydrogel: synthesis, characterization and antibacterial study. Carbohydr. Polym. 89, 906–913.

Khaskheli, A.A., Talpur, F.N., Ashraf, M.A., Cebeci, A., Jawaid, S., Afridi, H.I., 2015. Monitoring the *Rhizopus oryzae* lipase catalyzed hydrolysis of castor oil by ATR-FTIR spectroscopy. J. Mol. Catal. B Enzym. 113, 56–61. http://dx.doi.org/10.1016/j.molcatb.2015.01.002.

Kiyani, S., Ahmad, M., Zafar, M.A., Sultana, S., Khan, M.P.Z., Ashraf, M.A., Hussain, J., Yaseen, G., 2014. Ethnobotanical uses of medicinal plants for respiratory disorders among the inhabitants of Gallies–Abbottabad, Northern Pakistan. J. Ethnopharmacol. 156, 47–60. http://dx.doi.org/10.1016/j.jep.2014.08.005.

Lai, F.K., Li, H., 2011. Transient modeling of the reversible response of the hydrogel to the change in the ionic strength of solutions. Mech. Mater. 43, 287–298.

Li, S.F., Yang, Y.J., Li, H.B., Yang, X.L., Xu, H.B., 2007. PH-responsive semi-interpenetrating networks hydrogels of poly(-acrylic acid-acrylamide-methacrylate) and amylase. J. Appl. Polym. Sci. 106, 3792–3799.

Li, B.L., Lu, X.L., Ma, Y.H., Chen, Z., 2014. Thermo- and pH-responsive behaviors of aqueous poly(acrylic acid)/poly(4-vinylpyridine) complex material characterized by ATR-FTIR and UV–Vis spectroscopy. Eur. Polym. J. 60, 255–261.

Liu, C.H., Chen, Y.Q., Chen, J.G., 2010. Synthesis and characteristics of pH-sensitive semi-interpenetrating polymer network hydrogels based on konjac glucomannan and poly(aspartic acid) for in vitro drug delivery. Carbohydr. Polym. 79, 500–506.

Mandal, B., Ray, S.K., 2014. Swelling, diffusion, network parameters and adsorption properties of IPN hydrogel of chitosan and acrylic copolymer. Mater. Sci. Eng. C 44, 132–143.

Matsuyama, M., Kokufuta, E., Kusumi, T., Harada, K., 1980. On the poly(beta-DL-aspartic acid). Macromolecules 13, 196–198.

Mehr, M.J.Z., Pourjavadi, A., Salimi, H., Kurdtabar, M., 2009. Protein- and homo poly(amino acid)-based hydrogels with super-swelling properties. Polym. Adv. Technol. 20, 655–671.

Naureen, R., Tariq, M., Yusoff, I., Choudhury, A.J.K., Ashraf, M.A., 2014. Synthesis, spectroscopic and chromatographic studies of sunflower oil biodiesel using optimized base catalyzed methanolysis. Saudi J. Biol. Sci. 22, 322–339. http://dx.doi.org/10.1016/j.sjbs.2014.11.017.

Rajapakse, R.M.G., Tennakoon, D.T.B., Perera, J.S.H.Q., Bandara, W.M.A.T., Krishantha, D.M.M., 2005. Electrochemical impedance

spectroscopic and other studies of polyaniline–montmorillonite intercalates. J. Compos. Mater. 39, 1985–1999.

Ruiz-Rubio, L., Vilas, J.L., Rodríguez, M., Leon, L.M., 2014. Thermal behaviour of H-bonded interpolymer complexes based on polymers with acrylamide or lactame groups and poly(acrylic acid): influence of N-alkyl and a-methyl substitutions. Polym. Degrad. Stab. 109, 147–153.

Safi, S.Z., Qvist, R., Chinna, K., Ashraf, M.A., Paramasivam, D., Ismail, I.S., 2015. Gene expression profiling of the peripheral blood mononuclear cells of offspring of one type 2 diabetic parent. Int. J. Diabetes Dev. Ctries 1, 1–8. http://dx.doi.org/10.1007/s13410-015-0369-1.

Surhio, M.A., Talpur, F.N., Nizamani, S.M., Amin, F., Bong, C.W., Lee, C.W., Ashraf, M.A., Shahd, M.R., 2014. Complete degradation of dimethyl phthalate by biochemical cooperation of the *Bacillus thuringiensis* strain isolated from cotton field soil. RSC Adv. 4, 55960–55966.

Vudjunga, C., Chaisuwana, U., Pangana, U., Chaipugdeea, N., Boonyoda, S., Santawiteeb, O., Saengsuwana, S., 2014. Effect of natural rubber contents on biodegradation and water absorption of interpenetrating polymer network (IPN) hydrogel from natural rubber and cassava starch. Sci. Direct Energy Proc. 56, 255–263.